On the atomic structure of $Zr_{60}Cu_{20}Fe_{20}$ metallic glass

I Kaban[1], P Jóvári[2], M Stoica[1], N Mattern[1], J Eckert[1,#], W Hoyer[3], B Beuneu[4]

[1]IFW Dresden, Institute for Complex Materials, P.O. Box 270116, D-01171 Dresden, Germany
[2]Research Institute for Solid State Physics and Optics, H-1525 Budapest, POB 49, Hungary
[3]Institute of Physics, Chemnitz University of Technology, D-09107 Chemnitz, Germany
[4]Laboratoire Léon Brillouin, CEA-Saclay 91191 Gif sur Yvette Cedex France
[#]Also at TU Dresden, Institute of Materials Science, D-01062 Dresden, Germany

E-mail: i.kaban@ifw-dresden.de

Abstract

The structure of $Zr_{60}Cu_{20}Fe_{20}$ metallic glass has been studied with high-energy x-ray diffraction, neutron diffraction and extended x-ray absorption spectroscopy and modelled with the reverse Monte-Carlo simulation technique. It is found that Cu and Fe atoms prefer Zr as a nearest neighbour. The mean interatomic distance between Cu/Fe and Zr atoms in the glass is remarkably shorter than the sum of the respective atomic radii. The coordination numbers for Cu/Fe-Cu/Fe pairs are very close to each other suggesting a regular distribution of Cu and Fe atoms in the $Zr_{60}Cu_{20}Fe_{20}$ metallic glass.

PACS numbers: 61.43.Dq, 61.05.cp, 61.05.fm, 61.05.cj

1. Introduction

Glass formation in the Cu-Fe-Zr ternary system and in the $Zr_{60}Cu_{20}Fe_{20}$ alloy in particular has been studied earlier [1-4]. The $Zr_{60}Cu_{20}Fe_{20}$ composition is important because it provides a base for the quaternary bulk metallic glasses in the $(Zr_xCu_{100-x})_{0.8}(Fe_{40}Al_{60})_{0.2}$ system reported recently [5]. These glasses are interesting for biomedical applications, for example as implants. The interest in this system is also caused by the principal difference between the binary system Cu-Fe and the other two systems (Cu-Zr and Fe-Zr) limiting the concentration triangle Cu-Fe-Zr. The binary systems Cu-Zr and Fe-Zr are characterized by a negative heat of mixing and formation of a series of binary compounds and eutectic alloys in the crystalline state [6,7]. Both Cu-Zr and Fe-Zr binary systems demonstrate a high glass-forming ability [8-13]. In contrast, the heat of mixing of the Cu-Fe binary system is positive and the mutual solubility of Cu and Fe is very low in the solid state [6,7]. There is a liquid-liquid miscibility gap in the supercooled Cu-Fe liquids [14]. Cu-Fe alloys show almost zero glass-forming ability. Formation of an amorphous phase has only been reported for the thin Cu-Fe films (about 60 nm thickness) upon application of high energy (300 keV) ion mixing [15].

Inoue et al [1] found that there is a two-stage endothermic reaction for $Zr_{70}(Cu\text{-}Fe)_{30}$ metallic glasses upon annealing at temperatures below the glass transition temperature T_g. This was explained

by the difference in the bonding among the constituent elements and the differences in the atomic rearrangements by the structural relaxation. The low-temperature endothermic peak was attributed to local and medium-range rearrangements of Cu and Fe atoms with weak bonding, while the high-temperature endothermic reaction was related to the long-range co-operative regroupings of Cu-Zr and Fe-Zr pairs.

Michaelsen et al [2] studied Zr-rich $Zr_{100-x}(Cu\text{-}Fe)_x$ ($24 \leq x \leq 50$) metallic glasses with different Cu-Fe ratio by means of Mössbauer spectroscopy. Based on the analysis of the experimental spectra it was suggested that Fe atoms prefer Zr as nearest neighbours similar to the short-range ordering in the binary Zr_2Fe amorphous phase, i.e. in other words, Fe was concluded to not substitute for Cu isostructurally in the Zr-rich ternary glasses. Zhou et al [3] observed that X-ray photoelectron spectra (XPS) of ternary $Zr_{76}(Fe_xCu_{1-x})_{24}$ metallic glasses can be roughly decomposed into two independent contributions from the state of the respective binary metallic glasses Zr-Fe and Zr-Cu, which might be interpreted as an evidence of phase separation in the ternary Zr-Cu-Fe metallic glasses. However, it was also found in [3] that the shift of the binding energy of the Cu $2p_{3/2}$ core level in Zr-Cu-Fe glasses increases with decreasing Cu concentration, which is opposite to what was observed for binary Zr-Cu glasses. Therefore, it can be supposed that the chemical environment around atoms in the ternary Zr-Cu-Fe metallic glasses differs from those in the Zr-rich binary Zr-Cu and Zr-Fe glasses.

In order to elucidate how the differences in bonding forces between Cu, Fe and Zr atoms in the corresponding pairs are reflected in the local atomic ordering in the ternary Zr-Cu-Fe metallic glasses, the six partial pair distribution functions should be known. In the present work, we investigate the $Zr_{60}Cu_{20}Fe_{20}$ metallic glass with the X-ray diffraction (XRD), neutron diffraction (ND) and extended X-ray absorption fine structure (EXAFS) experiments and model its structure with the reverse Monte Carlo (RMC) simulation method. Simultaneous modelling of the four experimental datasets allows to obtain partial pair distribution functions and to extract information on the short-range atomic order in the $Zr_{60}Cu_{20}Fe_{20}$ metallic glass.

2. Experimental

A master alloy with nominal composition $Zr_{60}Cu_{20}Fe_{20}$ was prepared by arc melting of a mixture of pure Cu (99.99%), Fe (99.95%), and Zr (99.96%) under a Ti-gettered Ar atmosphere. The alloy ingot was re-melted several times to ensure homogeneity. Amorphous ribbons (width of 4 mm, thickness of about 20 μm) were obtained by single-roller melt spinning on a copper wheel under Ar flow at 24 ms^{-1} tangential wheel velocity.

The x-ray diffraction experiment was performed at the BW5 beamline [16] at HASYLAB (DESY, Hamburg, Germany) with an energy of the incident beam of 100 keV. The scattered intensity

was recorded by a Ge solid-state detector. The raw data were corrected for background, polarization, detector dead-time and variations in detector solid angle [17].

The neutron diffraction measurement was carried out with the 7C2 diffractometer at the Léon Brillouin Laboratory (CEA-Saclay, France). The wavelength of the incident radiation was 0.73 Å. Pieces of amorphous ribbons were filled into a thin-walled (0.1 mm) vanadium container of 7 mm diameter. The raw data were corrected for the detector efficiency and background scattering. Attenuation due to the sample absorption was estimated according to [18].

The EXAFS measurements at the Cu and Fe *K*-absorption edges were carried out at the HASYLAB beamline X [16]. The spectra were collected in the transmission mode using fixed exit double-crystal Si(111). The intensities before and after the sample as well as after the reference samples were recorded by three ionization chambers filled with a mixture of Ar/N_2 (~10% absorption), Ar (~50% absorption) and Kr (~100% absorption), respectively. The x-ray absorption cross sections $\mu(E)$ were converted to $\chi(k)$ by standard procedures of data reduction using the program VIPER [19].

The experimental XRD and ND structure factors as well as k^3 weighted EXAFS $\chi(k)$ curves are shown in Fig. 1.

3. Results and discussion

The reverse Monte Carlo simulation technique [20, 21] has been successfully applied in a number of studies carried out on liquid and amorphous alloys. In this method, large-scale atomic models compatible (within experimental uncertainty) with experiments and physical constraints (e.g. density, coordination constraints) are generated (for details, see for example [11,21-24]). In the present work, the rmc++ program [21,25] has been used. The simulation box contained 24000 atoms with the proper stoichiometry. The number density of the system was 54.16 nm^{-3} calculated from the mass density 7.07 g/cm^3. EXAFS backscattering coefficients needed to obtain the model $\chi(k)$ functions were calculated by the FEFF8.4 program [26].

Four structural models have been tested for the $Zr_{60}Cu_{20}Fe_{20}$ metallic glass. In *Model 1*, it was supposed that Zr, Cu and Fe atoms can be bonded in any proportion, i.e. no restrictions on the topological and chemical order were used. In this model, the following minimum interatomic distances (cut offs) were applied: $r_{ZrZr}^{\min} = 2.8$ Å, $r_{ZrCu}^{\min} = r_{ZrFe}^{\min} = 2.4$ Å, $r_{CuCu}^{\min} = 2.2$ Å, $r_{CuFe}^{\min} = 2.2$ Å, $r_{FeFe}^{\min} = 2.1$ Å. In the next two models, the possibility of demixing in the $Zr_{60}Cu_{20}Fe_{20}$ glass was checked. In the *Model 2*, a coordination constraint prohibiting some part of Zr atoms to have simultaneously Cu and Fe nearest neighbours was applied. In the *Model 3*, formation of Cu-Fe pairs was completely forbidden by increasing the Cu-Fe cut off up to 3.1 Å. Finally, in the *Model 4*, a coordination constraint determining that Fe atoms are coordinated only by Zr atoms was used (that is, besides Fe-Cu, Fe-Fe pairing was also forbidden).

Initial configurations were obtained by putting atoms randomly in the simulation box. In the next step, the atoms were moved around to satisfy the cut offs. Then the experimental diffraction datasets were fitted and coordination constraints were introduced if needed. The EXAFS spectra were added only in the final step. An important difference of diffraction and EXAFS is that the latter is a short range order technique insensitive to long range order fluctuations (and density). For this reason, if fitted simultaneously, it usually happens that convergence is already reached for EXAFS while the fit of diffraction datasets is still poor. Thus, some time can be saved if only diffraction data are fitted first (together with coordination constraints which may also influence long range order); EXAFS measurements are added if diffraction data are well reproduced and coordination constraints are satisfied.

A new feature of the rmc++ program [21,25] is the possibility of swapping two atoms at an arbitrary separation. Such moves are especially useful if there are long range correlations in the system or the packing fraction is high hindering the move of atoms. Swap moves were used in all simulation runs.

Some test runs were also carried out in this work to judge the relative importance of each experimental dataset. It was found that Zr-Zr and Zr-(Cu,Fe) correlations can only be reliably separated if both diffraction datasets are fitted. To resolve Zr-Cu and Zr-Fe correlations it was necessary to fit both EXAFS datasets.

As an example, the model curves obtained by the *Model 1* are compared with the experimental data in Fig. 1. It should be noted that similar quality fits were obtained also for the *Model 2* and *Model 3*. The quality of the fits became remarkably worse for the *Model 4* (not shown); therefore this model assuming that Fe atoms are bonded only to Zr atoms can be omitted from further discussion.

Figure 2 compares the partial pair distribution functions $g_{ij}(r)$ for the $Zr_{60}Cu_{20}Fe_{20}$ metallic glass obtained with the *Models 1-3*. It can be seen that the Cu-Cu, Cu-Fe and Fe-Fe partial pair distribution functions get an unusual shape if Cu-Fe bonds are forbidden. They do not oscillate around unity. Therefore, the *Model 3* prohibiting direct Cu-Fe bonding does not look as a plausible one. A similar behaviour of the Cu-Cu, Cu-Fe and Fe-Fe partial pair distribution functions has been observed for the *Model 2* upon strengthening of the coordination constraint that forced a part of the Zr atoms to have only Cu or Fe nearest neighbours. It is seen that already for 20% constraint, the Cu-Fe pair distribution function turns somewhat below the unity line, while the Fe-Fe pair distribution function goes above the unity line. Hence, if there is a tendency of separation of Cu and Fe atoms in the $Zr_{60}Cu_{20}Fe_{20}$ metallic glass, it is rather weak. Much more plausible is the *Model 1*, which enables all atomic bonds in the simulation box.

The nearest neighbour distances r_{ij} (uncertainty of about 0.02 Å) and the coordination numbers N_{ij} (uncertainty of about 10%) extracted from the *Model 1* and *Model 2* are listed in Table 1. As the difference between the coordination numbers corresponding to these models is rather small, only *Model 1* is further discussed. The mean interatomic distances r_{ZrFe} (2.67 Å) and r_{ZrCu} (2.78 Å) in the

$Zr_{60}Cu_{20}Fe_{20}$ metallic glass are remarkably shorter than the respective sums of the Goldschmidt atomic radii (r_{ZrFe} = 2.841 Å and r_{ZrCu} = 2.878 Å [27]). The same conclusion was made in the recent work of Michalik et al [27] who studied $Zr_{60}Cu_{20}Fe_{20}$ metallic glass by using X-ray diffraction (XRD) technique. Their analysis of the total radial distribution function revealed that the Zr-Fe and Zr-Cu interatomic distances in the glass are significantly shorter than the respective sums of the nominal atomic radii and than the interatomic distances in the crystalline state. It has also been established in other studies that the bond lengths between atoms of different type (e.g. metal and transition metal (TM), metal-semimetal) are significantly shorter in liquid or amorphous alloys as compared to their crystalline counterparts or the arithmetic sum of the respective atomic radii (see, for example, references 10,22,23). The strong affinity between Zr and TM atoms correlates with the enthalpy of mixing in the Zr-Cu and Zr-Fe binary systems [7]. The Cu-Cu, Cu-Zr and Zr-Zr interatomic distances in the ternary $Zr_{60}Cu_{20}Fe_{20}$ glass agree with those in the binary $Zr_{65}Cu_{35}$ glass [11] (Table 1). The mean Cu-Cu (2.60 Å) and Fe-Fe (2.53 Å) distances in the glassy $Zr_{60}Cu_{20}Fe_{20}$ are shorter than those in the crystalline $Zr_{60}Cu_{20}Fe_{20}$ (2.64 and 2.68 Å respectively [27]). This can be explained by densification of the atomic packing in the amorphous state.

It follows from the *Model 1* that Cu and Fe atoms are bonded to Zr atoms in approximately equal proportion (N_{ZrCu}=2.3, N_{ZrFe}=2.0). The mean coordination numbers for Cu/Fe-Cu/Fe pairs are very close to each other ($N_{ij}\approx 2$ for i,j = Cu,Fe) suggesting an even distribution of Cu and Fe atoms in the $Zr_{60}Cu_{20}Fe_{20}$ metallic glass on the large scale.

Conclusions

Four experimental datasets obtained for $Zr_{60}Cu_{20}Fe_{20}$ metallic glass (XRD, ND and EXAFS at Cu and Fe K-edges) were modelled simultaneously by the means of the reverse Monte Carlo simulation technique. Four different models have been tested. The model assuming an even distribution of the constituent atoms in the glass seems to be the most plausible. It is found that Cu and Fe atoms prefer Zr as nearest neighbours. They are bonded to Zr atoms in approximately equal proportion. The mean interatomic distance between Cu/Fe and Zr atoms in the $Zr_{60}Cu_{20}Fe_{20}$ metallic is remarkably shorter than the sum of the respective atomic radii. Almost all interatomic distances in the glassy state are shorter than those in crystalline $Zr_{60}Cu_{20}Fe_{20}$. The strong affinity between Zr and Cu/Fe atoms correlates with the enthalpy of mixing in the Zr-Cu and Zr-Fe binary systems.

Acknowledgment

I. Kaban acknowledges Deutsches Elektronen-Synchrotron DESY (Hamburg, Germany) for the support of experiments performed at HASYLAB. P. Jóvári was supported by the Bolyai Research Fellowship of the Hungarian Academy of Sciences.

References

[1] Inoue A, Masumoto T and Chen H S 1985 *J. Mater. Sci.* **20** 4057

[2] Michaelsen C, Meyer M and Freyhardt H C 1990 *J. Appl. Phys.* **68** 269

[3] Zhou X Y, He Z He and Zhang Q R 1997 *J. Phys.: Condens. Matter* **9** 4139

[4] Wang T L and Li B X 2009 *J. Alloys and Comp.* **481** 156

[5] Jin K and Löffler J F 2005 *Appl. Phys. Lett.* **86** 241909

[6] Massalski T B, Okamoto H, Subramanian P R and Kacprzak L (ed) 1990 *Binary Alloy Phase diagrams* (Materials Park, Ohio: ASM International)

[7] De Boer F R, Boom R, Mattens W C M, Miedema A R and Niessen A R 1989 *Cohesion in Metals: Transition Metal Alloys* (North-Holland Physics Publishing, Amsterdam, 1989)

[8] Ray R, Giessen B C and Grant N J 1968 *Scripta Metall.* **2** 359

[9] Altounian Z, Guo-Hua T, Strom-Olsen J O 1982 *J. Appl. Phys.* **53** 4755

[10] Buschow K H J 1984 *J. Phys. F : Met. Phys.* **14** 593

[11] Mattern N, Jóvári P, Kaban I, Gruner S, Elsner A, Kokotin V, Franz H, Beuneu B and Eckert J 2009 *J. Alloys and Comp.* **485** 163

[12] Masumoto T, Ohnuma S, Shirakawa K, Nose M and Kobayashi K 1980 *J. Phys. Colloq.* **41** 686

[13] Buschow K H J, Vincze I, van der Woude F 1983 *J. Non-Cryst. Solids* **54** 101

[14] Nakagawa Y 1958 *Acta Metall.* **6** 704

[15] Huang L J, Liu B X and Li H D 1987 *Appl. Phys. A: Solids Surf.* **44** 269

[16] http://www.hasylab.de

[17] Poulsen H F, Neumann H-B, Schneider J R, Neuefeind J and Zeidler M D 1995 *J. Non-Cryst. Solids* **188** 63

[18] Paalman H H and Pings C J 1962 *J. Appl. Phys*. **33** 2635

[19] Klementev K V 2001 *J. Phys. D: Appl. Phys.* **34** 209

[20] McGreevy R L and Pusztai L 1988 Mol. Simul. **1** 359

[21] Gereben O, Jóvári P, Temleitner L, Pusztai L 2007 *J. Optoelectron. Adv. Mater.* **9** 3021

[22] Jóvári P, Saksl K, Pryds N, Lebech B, Bailey N P, Mellergård A, Delaplane R G and Franz H 2007 *Phys. Rev.* B **76**, 054208

[23] Gruner S, Marczinke J, Hennet L, Hoyer W and Cuello G J 2009 *J. Phys.: Condens. Matter* **21** 385403

[24] Kaban I, Jóvári P, Stoica M, Eckert J, Hoyer W and Beuneu B 2009 *Phys. Rev.* B **79** (2009) 212201

[25] http://www.szfki.hu/~nphys/rmc++/opening.html

[26] Ankudinov A L, Ravel B, Rehr J J and Conradson S D 1998 *Phys. Rev.* B **58** 7565

[27] Michalik S, Saksl K, Sovák P, Csach K, Jiang J Z 2009 *J. Alloys and Comp.* 478 441

Table 1. Mean interatomic distances r_{ij} and coordination numbers N_{ij} for $Zr_{60}Cu_{20}Fe_{20}$ metallic glass. The error of r_{ij} is about 0.02 Å. The uncertainty of N_{ij} is about 10%. The structural parameters of $Zr_{65}Cu_{35}$ metallic glass [11] are given for comparison.

Pairs	$Zr_{60}Cu_{20}Fe_{20}$ metallic glass This study Model 1		$Zr_{60}Cu_{20}Fe_{20}$ metallic glass This study Model 2 (20% demixing)		$Zr_{65}Cu_{35}$ metallic glass [11]	
	r_{ij} (Å)	N_{ij}	r_{ij} (Å)	N_{ij}	r_{ij} (Å)	N_{ij}
Zr-Zr	3.17	8.9	3.17	9.2	3.16	9.4
Zr-Cu	2.78	2.3	2.78	2.3	2.80	3.7
Zr-Fe	2.67	2.0	2.67	2.1		
Cu-Zr	2.78	7.0	2.78	6.8	2.80	6.9
Cu-Cu	2.60	2.0	2.60	1.9	2.63	4.6
Cu-Fe	2.57	2.0	2.57	1.8		
Fe-Zr	2.67	6.0	2.67	6.4		
Fe-Cu	2.57	2.0	2.57	1.8		
Fe-Fe	2.53	1.7	2.53	1.6		

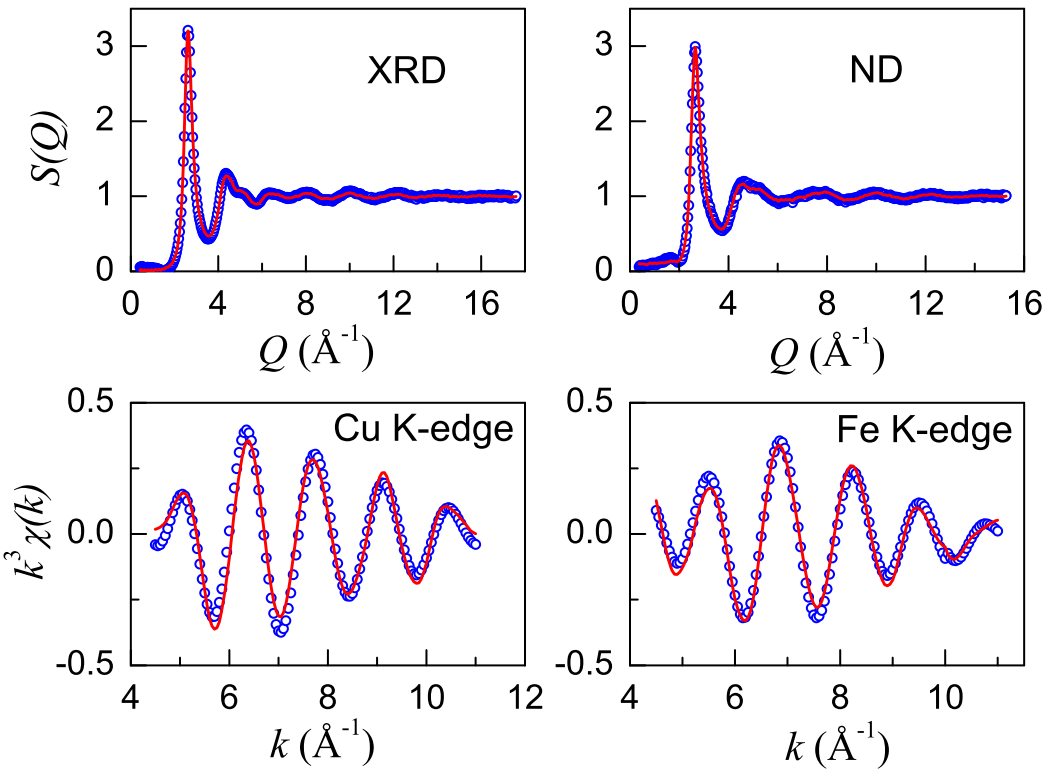

Figure 1. XRD and ND structure factors, and EXAFS spectra for $Zr_{60}Cu_{20}Fe_{20}$ metallic glass: c*ircles* – experimental data, *lines* – obtained by simultaneous RMC modelling of four measurements using *Model 1*.

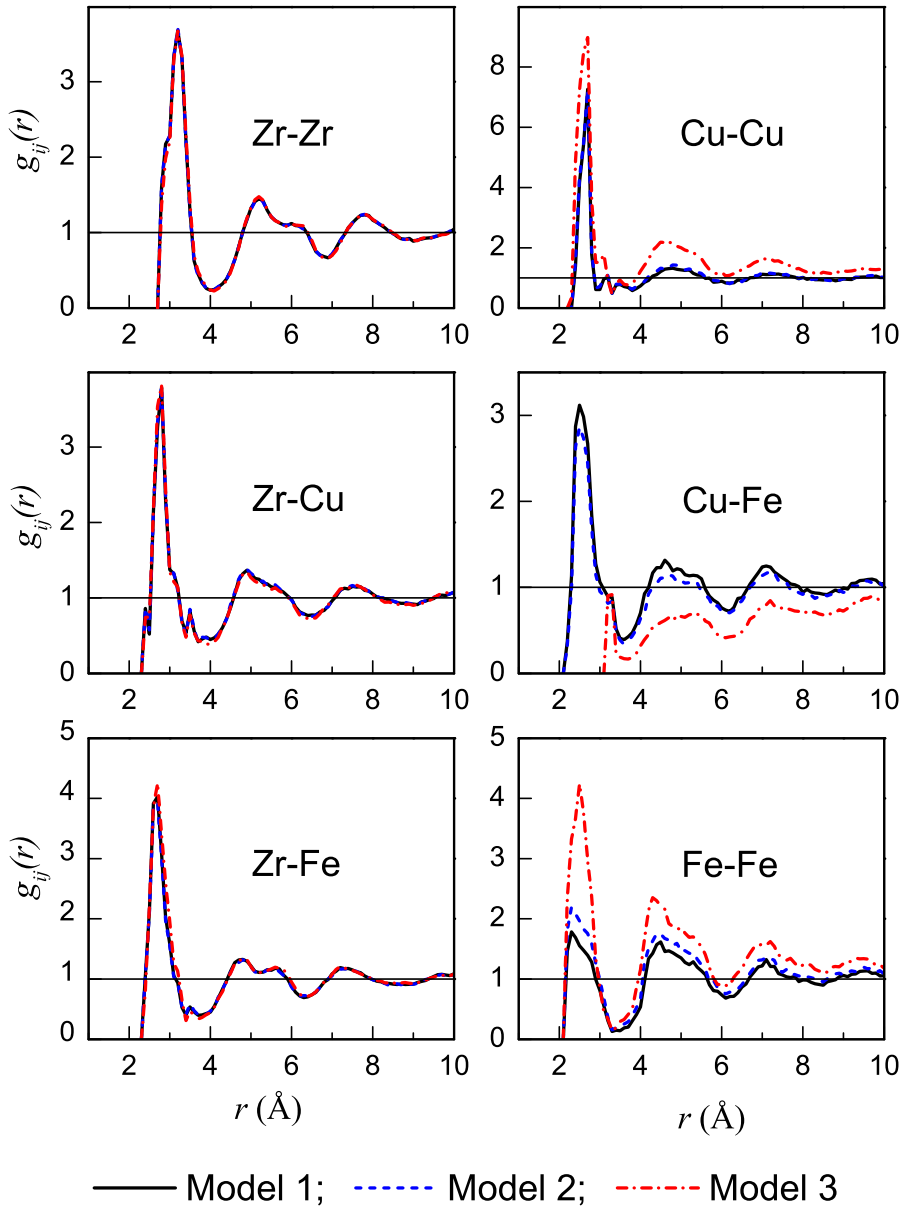

Figure 2. Partial pair distribution functions for the $Zr_{60}Cu_{20}Fe_{20}$ composition extracted from the RMC final simulation boxes obtained with different models. *Model 1* (*full line*) - all bonds are allowed, no coordination constraints are applied. *Model 2* (*dashed line*) - all bonds are allowed; coordination constraint: 20% of Zr atoms have only Cu neighbours and 20% of Zr atoms have only Fe neighbours. *Model 3* (*dash-dotted line*) - Cu-Fe bonds are forbidden. The Cu-Cu, Cu-Fe and Fe-Fe partial pair distribution functions get an unphysical shape if direct Cu-Fe bonds are forbidden.